



Structural, thermal, and mechanical characterisation of PEEK-based composites in cryogenic temperature

Maksim Nikonovich^{a,b,**}, Joana F.S. Costa^c, Ana C. Fonseca^c, Amilcar Ramalho^b, Nazanin Emami^{a,*}

^a Polymer-tribology Group, Division of Machine Element, Luleå University of Technology, Luleå, 97187, Sweden

^b CEMMPRE, Department of Mechanical Engineering, University of Coimbra, Portugal

^c CEMMPRE, Department of Chemical Engineering, University of Coimbra, Coimbra, Portugal

ARTICLE INFO

Keywords:

Polymer-matrix composites (PMCs)
Impact behaviour
Thermal properties
Fractography
Cryogenic temperature

ABSTRACT

Thermal, thermo-mechanical and mechanical properties of four different commercially available polyetheretherketones (PEEK) based materials were investigated. PEEK matrix was either modified and/or reinforced with carbon fibres, graphite and/or PTFE. Impact strength was measured at three different temperatures: 25 °C, –100 °C, and –195 °C. At 25 °C, thermal stability and mechanical properties, including the elastic modulus, compression, and impact strength, were enhanced with the addition of carbon fibres. Matrix modification had a minor impact on thermal stability, while the mechanical properties decreased, except for impact strength. At –100 °C, the mechanical properties of the neat polymers were improved, including increased impact strength by 20% compared to values at 25 °C. Addition of fillers hindered the rise of impact strength due to complex mechanisms caused by different coefficients of thermal expansion of reinforcements and matrix. At –195 °C, the significant increase of impact strength was revealed for unmodified PEEK reaching 30 times higher values than at 25 °C, while matrix modification suppressed the rise of impact strength. The scratch test indicated the superior behaviour of unfilled PEEK during the tested load range (up to 15 N), while the effect of the fillers was observed at much lower load threshold of 7 N.

1. Introduction

High performance thermoplastic materials are increasingly becoming a desirable alternative as materials of choice for components used in demanding environments, including low temperatures, vacuum conditions, and cryogenic liquids such as liquid nitrogen, natural gas and hydrogen [1–5]. In cryogenic environments, materials must show a high durability and operability under the simultaneous influence of low temperatures, changing pressures, and physical and chemical interactions with the environment. Moreover, in tribological applications, thermoplastic polymeric based materials have shown low friction and wear at low temperatures due to their self-lubricating properties, when the external lubrication with conventional greases and oils was not applicable [6–11].

The cryogenic properties of thermoplastic polymeric based materials include cryogenic mechanical properties, such as strength, modulus, impact strength, ductility, tribological and thermal properties such as

coefficient of thermal expansion (CTE) and thermal conductivity are important parameters for design-engineers in material selection phase [10,12,13].

In general, extreme low temperatures leads to some undesirable effects, for example, the decrease of impact strength and ultimate elongation [14]. At the same time, the modulus, hardness, creep, and fatigue resistance increase [13–16]. Particularly, Chu et al. [14] found that mechanical properties of 30% short glass fibre reinforced PEEK (tensile strength, tensile and flexural modulus, impact strength) were improved with the decrease of the temperatures from 295K to 20K. The authors concluded it was due to the thermal shrinkage of the polymer matrix that led to increased binding forces between molecules and enhanced glass fibre/matrix interface. At the same time, the more brittle fracture of the composite and the decrease of elongation at break were observed at cryogenic temperatures. The similar observations were made by Soleimani et al. [15], who investigated polypropylene (PP) reinforced with various amount of clay content (up to 5 wt%). The significant

* Corresponding author.

** Corresponding author. Polymer-tribology Group, Division of Machine Element, Luleå University of Technology, Luleå, 97187, Sweden.

E-mail addresses: maksim.nikonovich@ltu.se (M. Nikonovich), nazanin.emami@ltu.se (N. Emami).

<https://doi.org/10.1016/j.polymeresting.2023.108139>

Received 28 March 2023; Received in revised form 16 June 2023; Accepted 5 July 2023

Available online 6 July 2023

0142-9418/© 2023 The Authors. Published by Elsevier Ltd. This is an open access article under the CC BY license (<http://creativecommons.org/licenses/by/4.0/>).

improvement of the mechanical properties was found at cryogenic temperatures and with the addition of nanoclay. The increase of impact toughness with increasing nanoclay content was more noticeable at cryogenic temperature, than at room temperature. However, the obtained values of impact strength were generally lower for both neat PP and the nanocomposites at cryogenic temperature.

The ability of polymer molecules to experience low-temperature relaxations was also associated with improved ductility and toughness. Polyetheretherketones (PEEK) were found to become a suitable material of choice in tribological demanding applications at low temperatures, exhibiting superior damping capability and wear resistance at lower temperatures, compared to other materials [8,17–22]. Moreover, the thermal, mechanical and tribological behaviour of PEEK could be improved by using fibres, to increase the strength and modulus, and fillers such as graphite, polytetrafluoroethylene (PTFE) and MoS₂, to promote self-lubricity in the dry sliding contacts at both room and cryogenic temperatures [7,13,23,24]. However, some studies have reported a decrease in compression properties, impact strength and toughness due to the temperature effect and/or fibre orientation in reinforced PEEK composites [25–28]. Change of ambient temperature and structure of PEEK resulted in the alterations in fracture behaviour and toughening mechanisms. Moreover, the increase of strain rate changed the quasi-ductile fracture of PEEK matrix to a brittle failure mode, resulting in a significant decrease in toughness [25]. The tribological performance of PEEK and PEEK composites was primarily affected by their mechanical properties. It was found that the increased wear resistance in some type of wear mechanisms can be related to the decreased strength and toughness [29,30].

Despite extensive studies of PEEK composites at room temperature, the cryogenic mechanical properties of PEEK composites remain unexplored. Moreover, a number of research groups designs and produces thermoplastic polymers specially for applications at cryogenic temperatures, which structure and performance require additional development and investigation.

In the current work, relationship between mechanical and thermal properties of new PEEK based materials for cryogenic applications was studied. The newly developed PEEK based materials are either modified PEEK matrix and/or reinforced with carbon fibres, graphite and/or PTFE. Therefore, the main objectives of this research are: 1) to reveal the impact of the matrix modification and/or reinforcement on the mechanical and thermal properties of PEEK based composites at room and cryogenic temperatures; 2) to investigate the factors leading to the changes of the fracture mechanisms at cryogenic temperature versus at room temperature; 3) to study the intercorrelation of mechanical properties, particularly, impact strength, with thermomechanical properties (low temperature relaxation processes).

2. Materials

Four commercial PEEK-based composites were investigated based on their appropriate properties for tribological application: (i) neat PEEK as a reference material (PEEK1), (ii) a wear grade PEEK reinforced with carbon fibres, graphite and PTFE (PEEK2 d), (iii) a modified PEEK for cryogenic applications (PEEK3), (iv) a modified PEEK filled with PTFE (PEEK4). Commercial materials were supplied by Victrex, UK. The selected properties of the composites provided by the supplier are presented in Table 1.

3. Experimental details

3.1. Thermal properties

3.1.1. Differential Scanning Calorimetry

Differential Scanning Calorimetry (DSC) (Mettler Toledo AB, DSC821e) was performed to determine the glass transition temperature (T_g), melting temperature (T_m), and the degree of crystallinity (X_c) of the

Table 1

Selected thermal and mechanical properties of the studied commercially available PEEK-based materials provided by the supplier.

| Commercial material | Young's modulus, GPa | Flexural modulus, GPa | CTE, $10^{-6} K^{-1}$ | Charpy impact strength, $kJ m^{-2}$ | T_g , °C | T_m , °C |
|---------------------|----------------------|-----------------------|-----------------------|-------------------------------------|------------|------------|
| PEEK1 | 4 | 3.8 | 45 | 7 | 143 | 343 |
| PEEK2 | 13 | 11.5 | 45 | 5 | 143 | 343 |
| PEEK3 | – | 3.5 | 65 | – | 143 | 343 |
| PEEK4 | – | 3.3 | 65 | – | – | – |

specimens. The test samples weighted in the range of 9–11 mg. The DSC cycle comprised of three steps: dynamic (first heating), isothermal and second dynamic step that included cooling and second dynamic heating step. Details of the DSC cycle are presented in Table 2. Three repetitions of the DSC cycle were carried out for each material. Standard 70 μ l aluminium crucibles with a pierced lid were used. For some specimens, deconvolution of the resulting curve was done to separate the superimposed peaks. For this purpose, Pearson IV model was applied using PeakFit v4.12 software.

3.1.2. Thermogravimetric analysis

Thermogravimetric analysis (TGA) was carried out to evaluate the degradation temperature of the specimens in nitrogen atmosphere using a Netzsch TF 209F1 Libra. The specimens were heated from 25 °C to 800 °C at a heating rate of 10 °C·min⁻¹. Alumina crucibles were used with the test sample weight in the range of 8–11 mg. Three specimens per materials were analysed.

3.1.3. Dilatometry

Thermal expansion of the materials was measured using a dilatometer Netzsch DIC 402C, from 25 °C to 300 °C, at a heating rate of 5 °C·min⁻¹ in nitrogen gas atmosphere according to ASTM standard E831-19. The length of the test specimens ranged from 7 to 10 mm.

3.1.4. Dynamic mechanical analysis

Dynamic mechanical analysis (DMA) was performed on Triton 2000 DMA (Triton Technology, Ltd., UK) in a temperature sweep mode starting from –170 °C up to 300 °C with a heating rate of 2 °C·min⁻¹. The test samples were mounted in single cantilever configuration and tested at a frequency of 1 Hz.

3.2. Mechanical properties

Impulse excitation technique was used to measure modulus of elasticity and shear modulus of the specimens according to standard ASTM E1876-01. The specimens were 120 mm in length, 36 mm in width, and 6 mm in thickness. The specimen free vibrations were induced by the rapid impact of a steel ball and recorded by sensitive indicators. The data acquisition system was based on oscilloscope PicoScope 3204A together with PicoScope 6 software. The acquisition frequency was set to 20.8 kHz. Fast Fourier transform (FFT) algorithm was used to calculate the resonance frequency at both bending and torsion modes.

The compression testing was performed on the universal testing machine Instron according to standard ASTM D695-15. Specimens with dimensions of 12.7 × 12.7 × 25.4 mm³ were compressed in the

Table 2

Details of the DSC cycle used for specimen characterisation.

| Cycle steps | Heating rate, °C·min ⁻¹ | Temperature, °C | Time. min |
|-------------|------------------------------------|-----------------|-----------|
| 1st heating | 10 | 20–380 | – |
| Isotherm | – | 380 | 3 |
| 1st cooling | 20 | 380–90 | – |
| 2nd heating | 10 | 90–450 | – |

barrelling test without the addition of a lubricant between specimen and the plates at a speed of 1.3 mm min^{-1} . Five specimens of each material were tested.

Instrumented Charpy impact tests were performed on Instron CEAST 9050 pendulum impact testing machine according to standard ASTM D6110-03. The specimens with dimensions of $100 \times 12 \times 6 \text{ mm}^3$ and the machined V-shaped notch were fractured by an impact input energy of 25 J. Five repetitions of each test were completed.

3.3. Fractography

The surfaces after mechanical tests were examined by Scanning Electron Microscopy (SEM) (JEOL JSM-IT300) to study the fillers distribution and the matrix/reinforcement interface. To confirm the nature of reinforcement Energy-dispersive X-ray spectroscopy (EDS) was used.

3.4. Scratch test

Scratch test was conducted in two configurations using: 1) Vicker's indenter; 2) stainless steel ball SS 316L with a diameter of 10 mm. The normal load was proportionally increased with the tip moving. The scratch length was 6 mm, and the load range was between 0 and 15 N in both configurations accordingly. The scratch profiles were studied using white-light interferometry Zygo New View 7200 and a contact profilometer Mitutoyo SurfTest SJ-500.

4. Results and discussions

4.1. Thermal properties

4.1.1. Differential Scanning Calorimetry

Differential scanning calorimetry (DSC) results obtained during second heating cycle that include glass transition temperature (T_g), melting temperature (T_m) and degree of crystallinity of the specimens are presented in Table 3. Generally, it was observed that the matrix modification and/or reinforcement led to insignificant changes of the glass transition and melting temperatures of PEEK2, PEEK3 and PEEK4, compared to PEEK1. Particularly, the modification of the matrix decreased the melting temperature of PEEK3 to $339 \text{ }^\circ\text{C}$, while that of the PEEK1 was $343 \text{ }^\circ\text{C}$. Meanwhile, the addition of the reinforcements to PEEK1 matrix resulted in the decrease of the PEEK melting temperature of the composite PEEK2. A similar trend was found for the composite PEEK4. The obtained values of glass transition and melting temperatures are slightly different from those specified by the manufacturer, which was assumed due to inhomogeneous nature of the composites and impact of the manufacturing processes.

The degree of crystallinity (χ) of the materials was calculated using equation (1):

$$\chi_c (\%) = \frac{\Delta H}{\Delta H_{100}} \cdot 100, \# \quad (1)$$

where ΔH and ΔH_{100} are the experimental enthalpy of fusion calculated from the DSC curves and the theoretical enthalpy of fusion of 100% crystalline PEEK, respectively. The melting enthalpy of the 100% crystalline PEEK is 130 J g^{-1} [31]. The fillers wt% was deducted from the specimen weight prior to crystallinity calculation. Beforehand, in PEEK

Table 3
Crystallinity, glass transition and melting temperatures of PEEK in the studied materials at second heating cycle.

| Material | T_g , $^\circ\text{C}$ | T_m , $^\circ\text{C}$ | χ , % |
|----------|--------------------------|--------------------------|----------------|
| PEEK1 | 150.6 ± 0.6 | 342.1 ± 0.4 | 34.2 ± 0.7 |
| PEEK2 | 148.3 ± 0.9 | 341.7 ± 0.2 | 40.3 ± 0.6 |
| PEEK3 | 152.2 ± 0.2 | 339.9 ± 0.4 | 32.6 ± 1.0 |
| PEEK4 | 151.8 ± 0.8 | 339.1 ± 0.7 | 32.8 ± 2.1 |

2 and PEEK 4, the superimposed curves at melting temperature were deconvoluted. Based on reference [32], where a few methods were described and compared, Pearson IV model was chosen to be the most accurate.

The degree of crystallinity of the studied PEEK-based materials is summarised in Table 3. For the unfilled matrices, the percentage of crystallinity was approximately 33% showing no prominent effect of matrix modification. However, the addition of carbon fibres, increased significantly the degree of crystallinity of PEEK2, indicating that these acted as nucleation agents, as shown in previous studies [33]. The addition of PTFE, in turn, did not affect the degree of crystallinity of PEEK4 matrix, compared to PEEK3.

4.1.2. Thermogravimetric analysis

Thermogravimetric analysis (TGA) was carried out to study the thermal stability of the studied PEEK-based materials. The percentage of weight loss and its respective derivative, as a function of the temperature, are presented in Fig. 1. The characteristic degradation temperatures and residual weight (at $800 \text{ }^\circ\text{C}$) of the specimens are summarised in Table 4: the decomposition onset temperature (T_d) was referred to the beginning of the degradation process, T_5 , T_{10} and T_{20} were the temperatures of 5%, 10%, and 20% of the weight loss. The materials demonstrated two-step decomposition: the first pyrolysis stage was due to random chain scission of the ether and ketone bonds, started at T_d and followed by rapid mass loss at around $600 \text{ }^\circ\text{C}$; the second pyrolysis stage at above $630 \text{ }^\circ\text{C}$ was due to a slower volatilisation of formed residuals, which were more thermally stable [34–36]. It was clear that the PEEK modification had no influence on the thermal stability of the specimens, T_d of PEEK1 and PEEK3 was $579.1 \text{ }^\circ\text{C}$ and $576.6 \text{ }^\circ\text{C}$, respectively. Unlike, the addition of PTFE particles to PEEK matrix, in PEEK4 composite, initiated the thermal degradation at lower temperatures, $554.3 \text{ }^\circ\text{C}$, compared to PEEK1 due to lower degradation temperature of PTFE [37]. The first notable peak of weight loss observed at around $585 \text{ }^\circ\text{C}$ was attributed to maximum of PTFE volatilisation, followed by the second peak at around $600 \text{ }^\circ\text{C}$ due to highest decomposition rate of PEEK matrix (Fig. 1b). The similar behaviour was observed for PEEK2; however, the intensity of the peaks was the opposite to those observed for PEEK4 most likely due to a lower percentage of PTFE as reinforcement in PEEK2 composite. While the reinforcement with PTFE particles had a substantial effect on the degradation kinetics of PEEK4 specimen, on PEEK2 this effect was not so notorious. This fact can be due to the presence of carbon fibres and graphite in the composite, that contributed to the maintenance of the thermal stability of the composites. While the initial mass loss occurred at slightly lower temperature, the degradation onset temperature was slightly higher for the carbon fibre reinforced PEEK (PEEK2), in particular, $581.5 \text{ }^\circ\text{C}$, compared to PEEK1. The effect of the thermal stability became more evident at higher weight losses. Thus, weight losses at T_{10} and T_{20} increased by $5 \text{ }^\circ\text{C}$ and $7 \text{ }^\circ\text{C}$ with the addition of carbon fibres and graphite compared to unfilled PEEK1. A similar effect was found in the work by Li [38], where the short carbon fibres improved the thermal stability of the PEEK composites. The increased thermal stability was associated with the enhanced capacity of heat absorption of carbon fibres [39]. The maximum weight loss was reached at the higher temperature by $5 \text{ }^\circ\text{C}$ compared to PEEK1, having maximum weight loss at $597.5 \text{ }^\circ\text{C}$. Meanwhile, the reduction of the respective temperatures was approximately $20 \text{ }^\circ\text{C}$ with the addition of PTFE in PEEK4. However, the weight loss of PEEK4 was around 43% at the beginning of the second pyrolysis region, having the same values as PEEK1 and PEEK3.

4.1.3. Dilatometry

The linear thermal expansion coefficient (LCTE) (α) of the specimens measured from $25 \text{ }^\circ\text{C}$ up to $300 \text{ }^\circ\text{C}$ is presented in Fig. 2. LCTE of neat PEEK was calculated earlier and was $40\text{--}45 \times 10^{-6} \text{ K}^{-1}$, respectively [40]. To compare the LCTE of the specimens, the bulk material thermal expansion coefficient was calculated before glass transition temperature

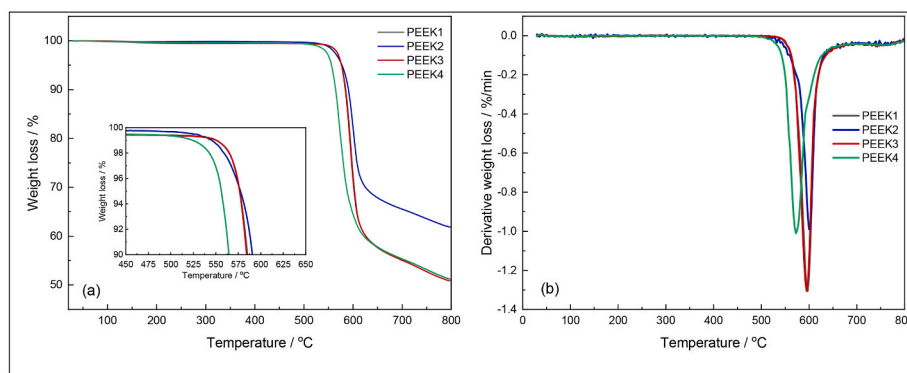


Fig. 1. TGA thermogram of the studied materials: (a) weight loss of the specimens as a function of the temperature, (b) derivative weight loss.

Table 4
Thermal degradation temperatures and residual weight of the studied materials, obtained from TGA.

| Specimen | T _d , °C | T ₅ , °C | T ₁₀ , °C | T ₂₀ , °C | Residual weight, % |
|----------|---------------------|---------------------|----------------------|----------------------|--------------------|
| PEEK1 | 579.1 ± 0.4 | 576.8 ± 0.7 | 585.2 ± 0.5 | 594.4 ± 0.6 | 50.9 ± 0.6 |
| | | | | | |
| PEEK2 | 581.5 ± 0.9 | 578.7 ± 1.5 | 590.8 ± 0.7 | 601.9 ± 1.0 | 62.3 ± 0.3 |
| | | | | | |
| PEEK3 | 576.6 ± 0.9 | 576.7 ± 0.6 | 584.0 ± 0.8 | 593.6 ± 0.6 | 51.6 ± 0.7 |
| | | | | | |
| PEEK4 | 554.3 ± 0.2 | 556.4 ± 1.8 | 564.1 ± 0.8 | 574.1 ± 2.3 | 52.1 ± 1.2 |
| | | | | | |

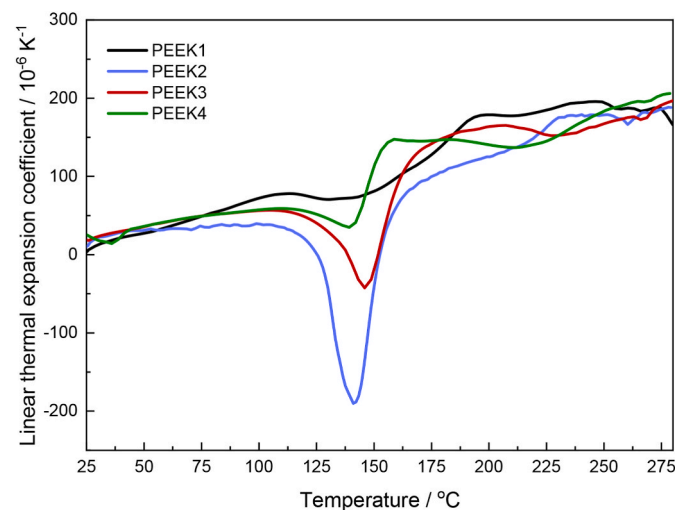


Fig. 2. Linear thermal expansion coefficient dependence on the temperature.

and after. In the present study, the LCTE of PEEK1 before glass transition temperature is $45.7 \times 10^{-6} \text{ K}^{-1}$, while the lower strain with LCTE value of $30.7 \times 10^{-6} \text{ K}^{-1}$ was observed for PEEK2 reinforced with carbon fibre, that has lower thermal expansion compared to the matrix. The modified matrix in PEEK3 showed slightly lower LCTE value of $42.4 \times 10^{-6} \text{ K}^{-1}$ in comparison to the PEEK1. However, the addition of PTFE, which is known to have a higher LCTE in PEEK4 increased the thermal expansion coefficient to approximately similar value of PEEK1 ($45.4 \times 10^{-6} \text{ K}^{-1}$).

Sufficient anisotropy of CTE was found in case of PEEK2 specimen, while no significant changes were found for other studied materials. The thermal expansion of PEEK2 measured in plane parallel to fibres orientation was revealed to be lower compared to PEEK1 since the fibres are mainly responsible for reduced strain which is in agreement with the

greater contraction reaching the glass transition temperature. While the polymer expansion showed to have the governing impact on LCTE in perpendicular direction.

As expected, the prominent change of LCTE was revealed near T_g due to the increase of chain mobility of the polymer. Moreover, at high temperature the strain is revealed to be dominant by the matrix, in particular, by the expansion of the amorphous phase, having approximately the same general trends for all four materials. The contraction of materials after reaching glass transition temperature was found at the thermal expansion graphs of modified and/or reinforced specimens. It was associated with the stress-relaxation induced by the manufacturing process of the PEEK composites and the presence of carbon fibres and/or PTFE particles [40–42].

4.1.4. Dynamic mechanical analysis

Dynamic mechanical analysis (DMA) was performed to determine the influence of the matrix modification and/or reinforcement on the viscoelastic properties of the studied materials. Fig. 3 shows the storage (E') and loss moduli (E'') of the polymers obtained in the temperature sweep mode (from -170 °C to 300 °C). The storage modulus, E', is related to the elastic energy reversibly stored in the sample, while the loss modulus, E'', shows the irreversible energy dissipation in the form of heat or the molecular rearrangement due to the plastic deformation. Two characteristic relaxations (α-relaxation or glass transition and β-relaxation due to relaxations in a backbone) were observed in the analysis of loss modulus curves. The temperatures defined from loss modulus curves at 1Hz for each of the materials, are summarised in

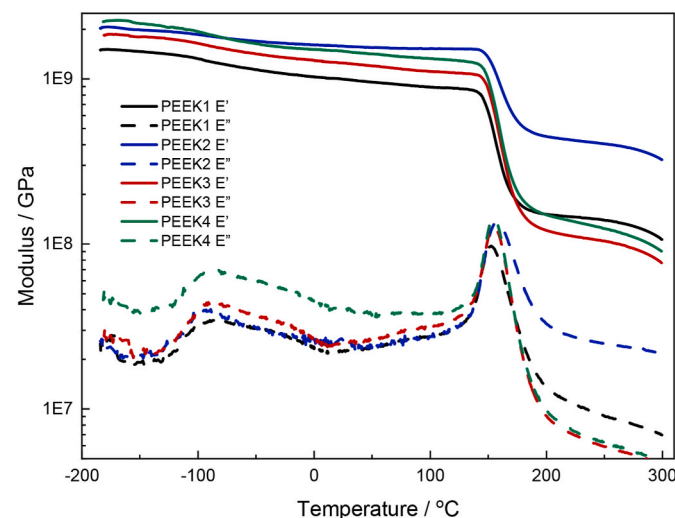


Fig. 3. Storage and loss modulus vs temperature curves for the studied materials.

Table 5
Storage modulus at various temperatures and glass transition temperatures of the studied materials.

| Material | E' @ -150 °C, GPa | E' @ -100 °C, GPa | E' @ 25 °C, GPa | E' @ 250 °C, GPa | α-relaxation, °C | β-relaxation, °C | tan δ @ 25 °C |
|----------|-------------------|-------------------|-----------------|------------------|------------------|------------------|---------------|
| PEEK1 | 1.47 | 1.33 | 1.00 | 0.14 | 152.3 | -85.18 | 0.020 |
| PEEK2 | 1.98 | 1.86 | 1.58 | 0.40 | 157.49 | -89.15 | 0.016 |
| PEEK3 | 1.80 | 1.65 | 1.25 | 0.10 | 154.83 | -88.65 | 0.019 |
| PEEK4 | 2.17 | 1.94 | 1.48 | 0.12 | 154.98 | -90.77 | 0.028 |

Table 5, and were found similar to values presented in the literature, moreover in some papers γ – relaxations (movement of pedant groups) were observed [8,17,18]. But in the present work, no such characteristic peaks were discovered.

With the increasing temperature, the storage modulus tends to decrease followed by a sudden decrease in the T_g region. The addition of stiffer carbon fibres and graphite increases the E' compared to PEEK1 (neat PEEK), maintaining the notable improvement in E' after reaching T_g region. In the case of PEEK3 and PEEK4, a higher loss on stiffness was observed, after the glass transition was reached. At low temperature, the increment of storage modulus was higher for PEEK1, PEEK3 and PEEK4, in comparison to PEEK2, most likely due to complexity of matrix shrinkage and reinforcement. The modification and/or reinforcement of the matrix have a pronounced constraining effect on the movement of the polymer chains, leading to an increase in E' , contrary to PEEK1. Consequently, after reaching the temperature of β -relaxation, the E' values of PEEK4 composite exceeded the value of E' of PEEK2 and reached 2.2 GPa at -150 °C, showing a combined outcome of matrix modification and PTFE reinforcement in PEEK4.

The T_g determined by DMA showed no significant differences for all materials and the results agreed with those obtained by DSC in this study. It is noteworthy that the T_g peak of PEEK1 and PEEK2 at high temperatures is slightly wider than that of PEEK3 and PEEK4, which in the case of composites with carbon fibres and graphite (PEEK2) is due to the reduction of the mobility of amorphous PEEK chains and higher degree of crystallinity [43]. In fact, the DSC results indicate a higher degree of crystallinity for PEEK2. Moreover, a small peak at 23.8 °C in loss modulus curves of PEEK2 and PEEK4 is associated with the β -relaxation of PTFE [8,42,43]. The highest values of loss modulus upon α -relaxation were observed for PEEK4 followed by PEEK2 and PEEK3, while the lowest value was obtained for PEEK1. The modification of the matrix and/or the reinforcement of the matrix had an effect on the viscosity of the polymers, since the molecular motion was restricted in the range of selected temperatures [44].

To better understand the effects of matrix modification and/or reinforcement on the behaviour of the composites, damping factor (tan

δ) was analysed (Fig. 4). As expected, the lowest tan δ for carbon fibre, graphite and PTFE reinforced composites PEEK2 was observed in the range of selected temperatures. The fibres contribute to a more effective stress distribution in the matrix, while the energy is mainly dissipated at the filler/matrix interface. Matrix modification of PEEK3 led to an increase in both storage and loss modulus, while the damping factor was similar to PEEK1, with the only notable change at the glass transition temperature, which showed the highest values. At the same time, the addition of PTFE particles to the modified matrix showed the highest damping effect, throughout the selected temperature range and became even more pronounced before reaching the glass transition temperature. At lower temperature, matrix shrinkage had a constraining effect on the molecular movement that resulted in increased materials' stiffness. At the same time, reinforcement of the matrix introduced thermal stress at matrix/filler interface. In case of PEEK4, due to discrepancy in CTE of the PEEK matrix and PTFE, the energy dissipation at the interface became more evident leading to higher damping. Whilst, reinforcing PEEK2 with carbon fibres and graphite, having a lower CTE compared to matrix, led to a reduction of damping due to improved matrix/filler interface as a result of matrix shrinkage.

4.2. Mechanical properties

Impulse excitation (IE) technique was used to measure the elastic (E) and the shear (G) modulus of the studied composites. The results are presented in Table 6. Generally, IE allows to determine the moduli through the analysis of resonant natural frequencies of vibration induced to the specimen by a pointed impact creating a sound wave. The results provided by the manufacturer (Table 1) were found to be similar to the ones obtained by IE. The matrix modification (PEEK3) had a minor effect on the Young's modulus and shear modulus, while the addition of PTFE particles to modified matrix (PEEK4) resulted in a decrease of stiffness and shear resistance compared to PEEK1. The addition of carbon fibres and/or graphite (PEEK2) had an opposite effect, notably improving the elastic modulus of the specimens.

Additionally, since polymer materials have a relatively high vibration damping factor and are linearly viscoelastic, the material damping might be described using a simple viscoelastic model, for example, the Kelvin-Voigt model. Therefore, applying Kelvin-Voigt model, the dissipation factor (tan δ) was calculated by equation (2):

$$\psi(t) = X e^{-\zeta \omega_n t} \cos(\omega_d t) \# \quad (2)$$

where X – maximum amplitude, ζ – damping coefficient ($\zeta = [\tan \delta]/2$), ω_n and ω_d – natural frequency and damping frequency respectively. The results are agreed with the general trends found during DMA.

Fig. 5 and Fig. 6 show the results of the compression strength and compression modulus of the four studied materials, respectively. The specimens were tested perpendicular to the fibres distribution plane, in

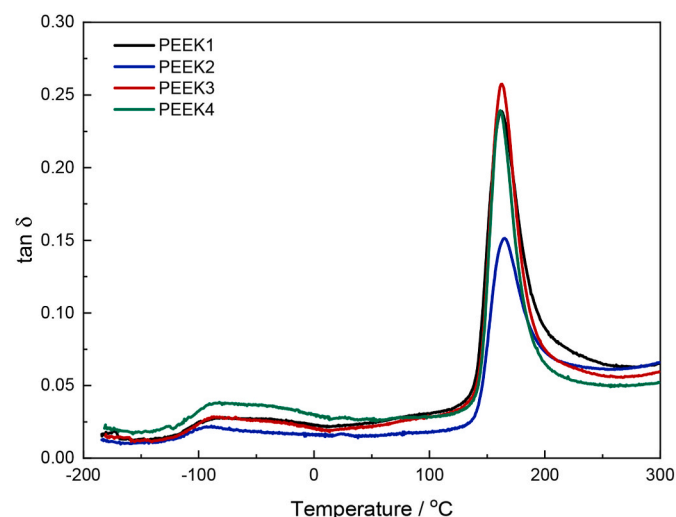


Fig. 4. Tan δ vs temperature curves of the studied commercial polymers.

Table 6
IE calculation results for the studied materials at 25 °C.

| Material | E, GPa | G, GPa | tan δ | Poisson ratio |
|----------|------------|------------|--------------|---------------|
| PEEK1 | 3.9 ± 0.2 | 1.4 ± 0.1 | 0.011 | 0.39 |
| PEEK2 | 11.7 ± 1.2 | – | 0.008 | – |
| PEEK3 | 3.8 ± 0.01 | 1.4 ± 0.01 | 0.011 | 0.36 |
| PEEK4 | 3.3 ± 0.2 | 1.2 ± 0.1 | 0.016 | 0.38 |

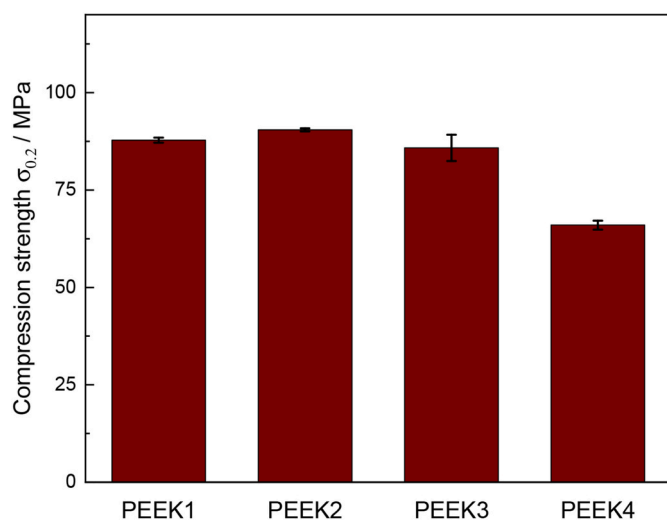


Fig. 5. The compression strength of the studied commercial materials.

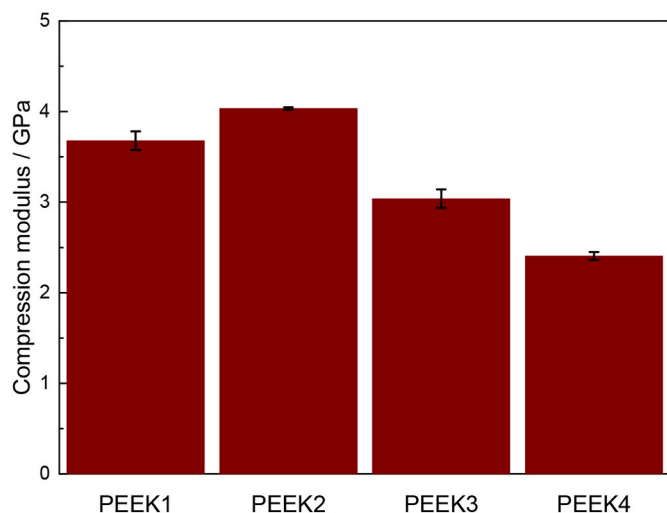


Fig. 6. The compression modulus of the studied commercial materials.

order to reveal the properties relevant to real tribological applications. For the three materials that were not filled with carbon fibre, the maximum compression strength could not have been obtained in the compression barreling test. These materials showed a ductile behaviour and were compressed to “pancake”-like state. To be able to compare all four materials, the yield compression strength at 0.002 strain was calculated. It is noteworthy that the addition of the carbon fibre as well as graphite in PEEK2 contributed to the increase of the yield compression strength up to 90 MPa, however, the material showed brittle fracture and the maximum value of the compression strength was calculated as 174 MPa. The matrix modification revealed to have a minor effect on the yield compression strength, while the addition of PTFE particles in PEEK4 composites decreased the strength down to 66 MPa. The results for the compression strength showed a comparable trend to the results for compression modulus, but the influence of the fillers and modification was found to be more notable on the compression modulus.

The measured mechanical properties are in a good agreement with the results obtained from DSC (Table 3). Compared to PEEK1 with compression modulus of 3.6 GPa, the matrix modification PEEK3 showed reduction in the compression modulus of the material down to 3 GPa. The lower degree of crystallinity of PEEK3 (32.6%) impacted the decrease of both compression strength by 3% and compressions modulus by 17%, compared to the respective values of PEEK1 with the

crystallinity of 34.2%. However, the addition of PTFE particles to modified PEEK matrix, PEEK4 (with the degree of crystallinity of 32.8%), reduced the compression strength by 24% and compression modulus by 33% (2.1 GPa). At the same time, the addition of carbon fibres that led to rise of PEEK crystallinity to 40% increased the modulus of PEEK2 by 14% (reaching 4.1 GPa) and compressive strength by 3%. This findings are also confirmed by other investigators, who found a relation between the mechanical and thermal properties of PEEK materials [45–47].

The significant difference in modulus obtained by impulse excitation technique and compression tests in PEEK2 is due to various testing modes. Previously, the significant influence of the fibre orientation on mechanical properties, including compression strength and compressions modulus was examined in study by Rasheva et al. [26]. It was found that there is a decrease of both properties if the fibres reinforcement plane was perpendicular to the compression direction, as in the present study.

Fig. 7 and Table 7 shows the results of Charpy impact test of the four studied PEEK-based materials at various temperatures, $-195\text{ }^{\circ}\text{C}$, $-100\text{ }^{\circ}\text{C}$, and $25\text{ }^{\circ}\text{C}$. Charpy impact tests revealed the primarily matrix dominant behaviour for all materials at tested temperatures. At room temperature ($25\text{ }^{\circ}\text{C}$) matrix modification increased the impact strength of PEEK3 (3.6 kJ/m^2) by 20% compared to PEEK1 (2.9 kJ/m^2). It might be clearly observed that the impact strength was notably improved by the addition of carbon fibres and graphite, reaching 5.3 kJ/m^2 . A similar effect was found for modified matrix reinforced with PTFE (PEEK4), increasing the impact strength up to 5.1 kJ/m^2 . Carbon fibres increased PEEK2 material capability to sustain the deformations at high strain rate increasing the impact energy absorbed by the material, due to the higher elastic modulus. Meanwhile, PEEK4 with a higher loss modulus, as it was revealed by DMA, showed better damping effect that, in turn, also resulted in higher impact strength.

At $-100\text{ }^{\circ}\text{C}$, the impact strength tended to slightly increase for unfilled materials as PEEK1 and PEEK3, however, a minor effect was observed in case of matrix modification, comparing to the rise of impact strength up to 3.7 kJ/m^2 for PEEK1. The addition of the PTFE particles to modified matrix (PEEK4) also significantly improved the impact strength at $-100\text{ }^{\circ}\text{C}$ compared to the other specimens. However, the gain was not substantial compared to the values at $25\text{ }^{\circ}\text{C}$, where the addition of carbon fibres, graphite and PTFE resulted in reduction of impact strength down to 4.9 kJ/m^2 . The temperature reduction to $-195\text{ }^{\circ}\text{C}$ resulted in the substantial rise of the impact energy for PEEK1 and PEEK2 based on the same matrix, 113 kJ/m^2 and 193 kJ/m^2 , respectively. Meanwhile, the unchanged behaviour was observed for the

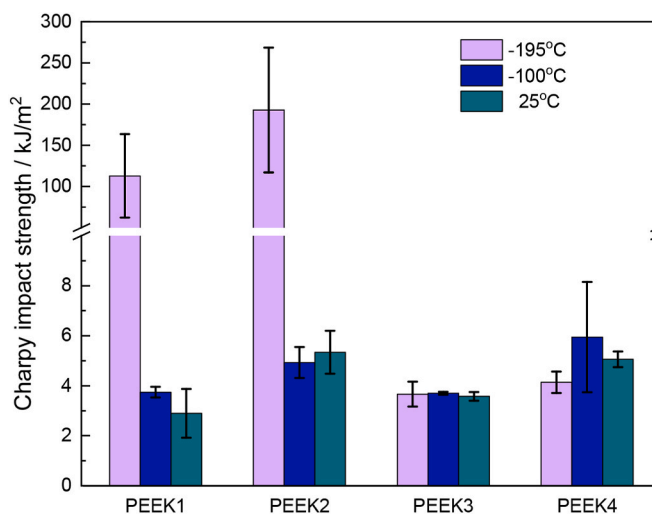


Fig. 7. Charpy impact strength of the studied materials measured at various temperatures.

Table 7
Impact strength (IS) of the studied materials at various temperatures.

| Material | IS @ -195 °C, kJ/m ² | IS @ -100 °C, kJ/m ² | IS @ 25 °C, kJ/m ² |
|----------|---------------------------------|---------------------------------|-------------------------------|
| PEEK1 | 112.9 ± 50.7 | 3.8 ± 0.2 | 2.9 ± 0.9 |
| PEEK2 | 192.8 ± 75.6 | 5.0 ± 0.6 | 5.3 ± 0.8 |
| PEEK3 | 3.7 ± 0.5 | 3.7 ± 0.1 | 3.6 ± 0.2 |
| PEEK4 | 4.1 ± 0.4 | 5.9 ± 2.2 | 5.1 ± 0.3 |

PEEK3 and PEEK4. PTFE in the studied materials tended to behave as glassy fillers having an insignificant effect on the polymer impact strength.

As it is known from literature, and can be seen from DMA data (Fig. 3 and, Table 5), the stiffness and the hardness of the materials is increasing significantly at low temperatures (below -50 °C) [14,16,48,49]. In this case, the elastic failure is most likely to happen since the kinetic energy of the impact stored elastically in the specimen until the limit of fracture toughness exceeded, while the plastic deformations are very limited. However, with increasing temperature, the energy dissipation occurs due to the plastic deformation of the polymer and becomes more pronounced. In the past works [19–21,50–52], the effect of low temperature and molecular relaxations on the impact strength of polymers was addressed, however, no direct correlation was established. Authors concluded that the temperature effect on the matrix behaviour might be a combination of several factors: damping factor, $\tan \delta$, and the blunting at the crack tip due to the adiabatic heating caused by the high strain rate. In the present study, a decrease, or at least unchanged behaviour, of the toughness was found at low temperature, while for some materials, the rapid increase in impact strength was also observed. According to Ref. [19], the $\tan \delta$ plays a major role, if the local temperature of polymer at the crack tip is below the glass transition. To calculate the effective temperature, equation (3) was used:

$$T_e = T_{am} + \Delta T \# \quad (3)$$

where T_{am} – is the test ambient temperature, and ΔT is the increase of temperature due to the heating induced by the impact, calculated by equation (4):

$$\Delta T = \frac{w_e}{\sqrt{\pi \rho c k t}} \# \quad (4)$$

For example, for PEEK1, the impact energy w_e at -100 °C is about 3.8 kJ/m². According to the commercial materials data sheets, the density of PEEK1 $\rho = 1.3 \times 10^3$ kg/m³, specific heat $c = 2.2$ kJ kg⁻¹ K⁻¹, thermal conductivity $k = 0.29 \times 10^{-3}$ kJ s⁻¹ K⁻¹ m⁻¹, and the impact time was assumed as 0.4 ms. As a result, the effective temperature was calculated as 18 °C. Therefore, it might be concluded that the thermal blunting of crack-tip affected the impact strength at 25 °C, however, at sufficiently low temperatures $\tan \delta$ plays a dominant role. The materials experienced the β -transition around -100 °C region, therefore, after the relaxation the polymer chains mobility was sufficiently reduced, which generally led to the small rise of the impact strength. At the same time, the competing mechanisms do not affect the impact strength significantly, compared to the values obtained at -100 °C, including the reduction of the yield stress with the increasing temperature and the thermal blunting of the tip to occur at 25 °C. In agreement with DMA results, the increased loss modulus supported the better absorption of the impact energy increasing the damping factor [19]. While the damping factor was higher for the PEEK4 composite, PEEK2 had the lowest damping due to the reduced molecular movement and the increased stiffness in the presence of carbon fibre. However, another mechanism was found to play a significant role in the reinforced materials attributed to the different thermal expansion coefficient of the constituents and the matrix. In this case, the reduction in impact strength of PEEK2 was due to the competitive mechanisms. On the one hand, the increase of $\tan \delta$ led to the increase of impact strength. On the other hand, graphite and fibres created the thermal stresses induced by

different thermal expansion coefficients, resulting in the small drop in the impact strength. At the same time, it is clear that the transition in impact strength cannot be accurately predicted by the location of the damping peaks, similar to findings in the past work [51], since the DMA measurements are conducted in the linear region with small deformations, while the impact tests connected to large deformations and ultimate properties of the polymers.

In the region of lower temperatures, after β -relaxation, it was found that the matrix modification tended to suppress the changes of the mechanical behaviour of PEEK3 and PEEK4 at -195 °C due to the absence of the any additional energy absorption process. In fact, the rapid increase of the Charpy impact strength was associated with either the increase of critical fracture stress or the ultimate elongation. With the decrease of temperature, the ultimate strain tends to decrease, however, the increase in mechanical properties at lower temperatures increase the maximum stresses, which in case of PEEK1 and PEEK2 was similar to quenching effect, creating the residual compressive stresses [53].

4.3. Fractography

Fig. 8 gives the examples of fractographies to reveal the influence of the temperature after Charpy impact test. Due to high strain rate deformation the PEEK matrices showed a brittle behaviour. At room temperature (25 °C) PEEK1 showed a typical river-like structure with severe plastic deformation sites representing the brittle behaviour of the material. PEEK3 fracture surfaces elucidated a self-toughening mechanism, including the micro-void coalescence and crack-tip blunting resulting in a smoother fracture surface, indicating quasi-brittle fracture. The addition of the fillers as for PEEK2 and PEEK4 created an extensive filler/matrix interface and resulted in a coarse fracture surface. The poor adhesion between the reinforcement (PTFE particles and carbon fibres) and matrix was revealed on the fracture surfaces for both composites, which promoted an additional stress-concentrations inside the matrix. The PEEK matrix itself also showed brittle behaviour in both composites. However, considering the higher impact strength of the composites compared to unfilled matrices, one assumption could be that such a weak interface creates a barrier for crack propagation and promotes higher energy absorption resulting in higher impact energy.

The decrease of temperature down to -100 °C slightly changed the morphology of the fracture surfaces. PEEK1 and unfilled modified PEEK3 were found to have the similar fracture surfaces. The river-like structure for PEEK3 materials was suggested due to increased critical fracture stress and hindering the intrinsic toughening mechanisms resulting in a brittle failure similar to the one observed for PEEK1 at 25 °C. PEEK1 fracture surface appeared to be smoother due to the limited plastic flow at the crack tip. PEEK2 demonstrated similar fracture surface to the one observed at room temperature and agreed with the values for the impact strength. However, the matrix/fibre interface was slightly improved, but the separation of carbon fibre from the polymer matrix and formation of voids because of detached PTFE particle still were observed. Similar morphology was found for PEEK4 composite. Although, like PEEK3, the fracture surface demonstrated brittle fracture with a fracture of a discrete PTFE particles wetted by the polymer matrix due to the matrix shrinkage.

The further reduction of temperature down to -195 °C revealed a notable change in fracture morphology of the studied composites. PEEK1 showed a smooth brittle fracture surface meaning the rapid cleavage crack propagation, characteristic for the elastic fracture. However, the modified PEEK3 fracture surface was found to be similar to the one observed for PEEK1 at -100 °C, sharing comparable respective values of the impact strength. Generally, the matrix modification shifted the transition impact strength to lower temperatures, compared to PEEK1. The rapid increase of the toughness was associated with the increased stiffness, hardness of the neat PEEK due the shrinkage and the prominent constrain of the polymer chains mobility after

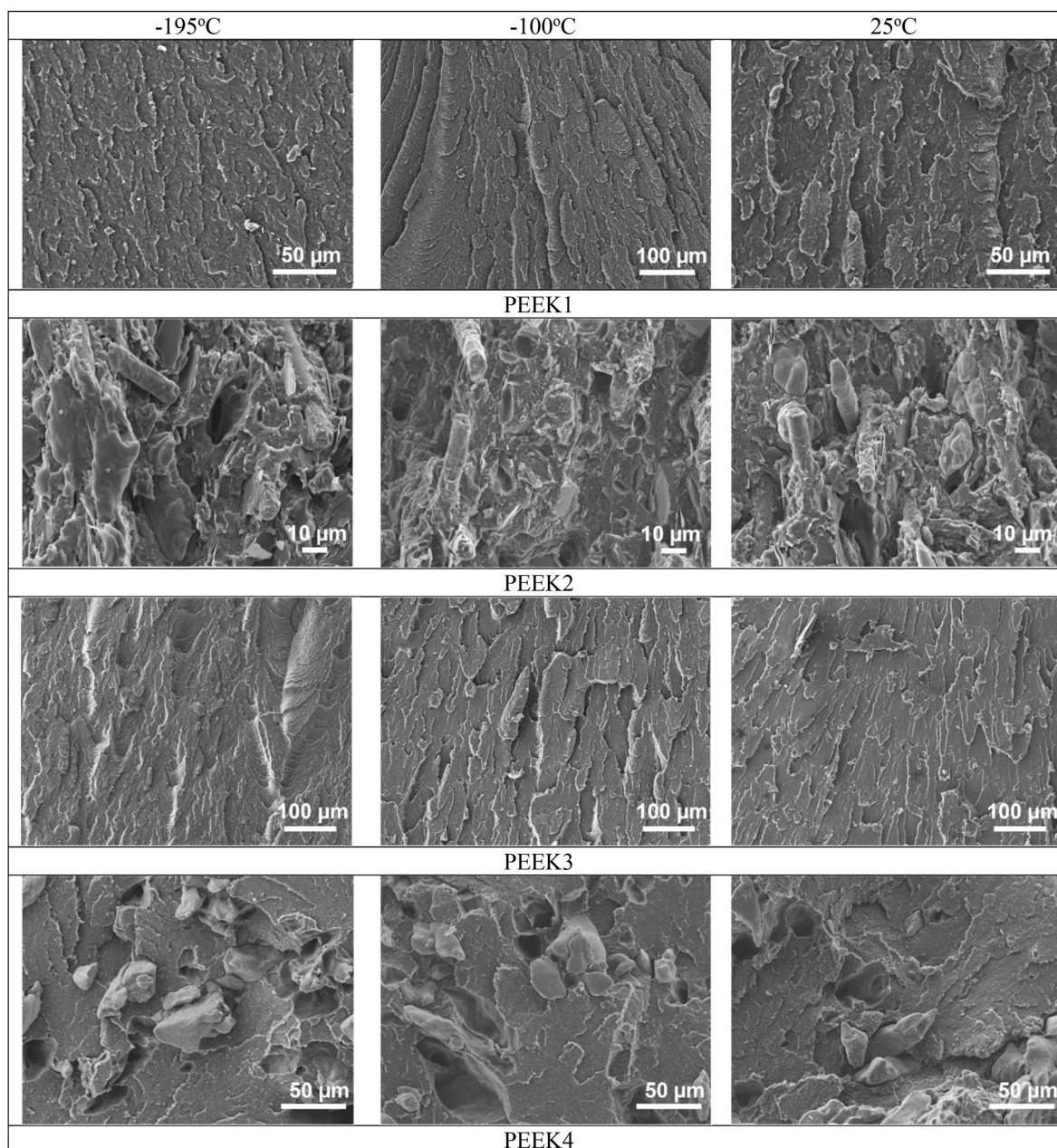


Fig. 8. Fracture surface of studied polymers obtained after failure in Charpy impact test at various temperatures.

β -relaxation. Reinforcements in PEEK2 composites appeared to be well adhered to matrix, improving significantly the matrix/fillers interface, due the matrix shrinkage. This resulted in better impact stress distribution among the matrix, and the fibres together with PTFE particles took a substantial part of the impact energy. While the crack propagated through graphite easy sheared pallets, the impact resistance of PEEK2 was mainly dominated by carbon cracking and fracture of PTFE particles. However, the detachment of individual PTFE particles still was observed. Another morphology was revealed for PEEK4 composites, showing the expressed brittle behaviour of the PEEK modified matrix and the separation of PTFE particles from the matrix, forming the voids.

4.4. Scratch test

To evaluate the influence of the fillers and matrix modification prior to tribological tests in future study, the scratch tests were conducted using two types of indenters: Vicker's indenter and stainless-steel ball

316L. In the test with Vicker's indenter friction was controlled by the mechanical strength of the materials, which influenced the plastic deformation at the surface shown in Fig. 9a. The instant friction was found to increase with the rise of applied load, also increasing the penetration depth of the indenter. The lower instant friction was found for the PEEK2 and PEEK1, which showed a higher modulus and compressive strength, while the modification made the polymer matrix softer and allowed the plastic flow, increasing the resistance to friction. After reaching 10 N, friction coefficient for all of the materials reached the plateau introducing the matrix dominant behaviour at higher loads. In the test with stainless ball friction was driven by the adhesive forces between ball and the materials surface (Fig. 9b). The friction coefficient was found to be independent to changing load for all of the studied materials. The lowest friction, approximately 0.02, was obtained for modified PEEK3, followed by PEEK4. PEEK2, reinforced with carbon fibres, graphite, and PTFE, had the sliding friction coefficient of 0.07. The matrix modification as in case of PEEK3 and PEEK4 suppressed the

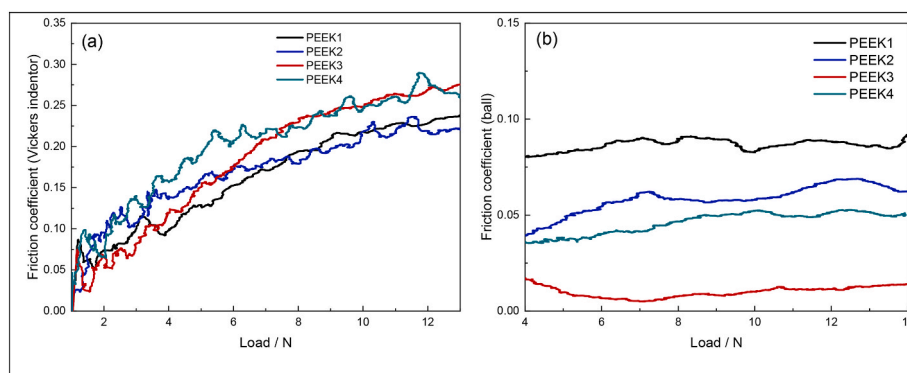


Fig. 9. Friction coefficient obtained by (a) Vicker's indenter and (b) stainless-steel ball scuffing against polymer surface.

adhesion of the polymer to the metal ball. Reinforcing the PEEK matrix with PTFE particles resulted in the increase of sliding friction. The addition of carbon fibre and graphite increased the stiffness of the material and decreased the real contact area, that led to a slight reduction of the adhesion between PEEK2 and the ball, compared to PEEK1.

Fig. 10 shows the representative scratch tracks for the studied materials, obtained by Vicker's indenter. For the unfilled PEEK, PEEK1 and PEEK3, the abrasive wear was dominated, however, the matrix was mostly ploughed away the track to the sides forming ploughing wedges. Scratches of the composites, PEEK2 and PEEK4, were revealed to be coarse with the presence of detached and/or cracked single fibres and PTFE particles. The modified matrix rupture might be also clearly seen on the scratch track of PEEK4 resulted in the friction coefficient fluctuation during Vicker's scratch test. Fig. 11 shows the amount of the materials removed from the wear track (scratched). Supported by the discussion before, the effect of the fillers is clearly observed under 7 N, while above that value, the increased amount of the material scratched away from the track. The slightly higher amount of wear was found for the modified unfilled polymer PEEK3 compared to neat PEEK1, although, it was following the same trend with changing load. However, the amount of the ploughed material was bigger for softer PEEK3 and PEEK4.

Basically, the wear of polymer composites includes few steps: matrix wear, filler wear and the matrix-filler interface delamination [26,27,30]. In case of weak matrix-filler interface, the third mechanism might dominate. For PEEK2, after a certain load, the fibres started to crack and peel off from the matrix. Therefore, the load support from the fibres is not available anymore, and the polymer can be easily worn off [27,54]. In PEEK4 composite, the PTFE particles can be easily removed from the matrix after the load reaching a certain limit and Vickers indenter penetrates to a certain depth (Fig. 10).

5. Conclusions

In this study, thermal, thermo-mechanical and mechanical properties

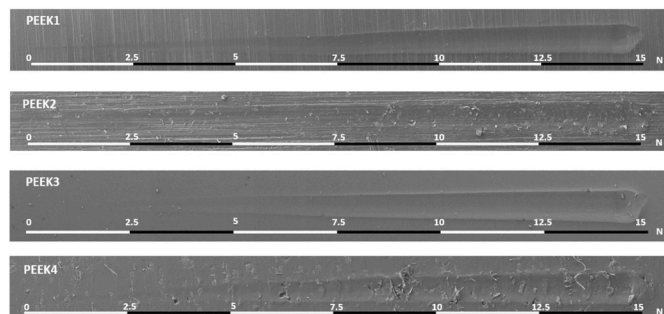


Fig. 10. SEM of the scratch tracks of the studied materials.

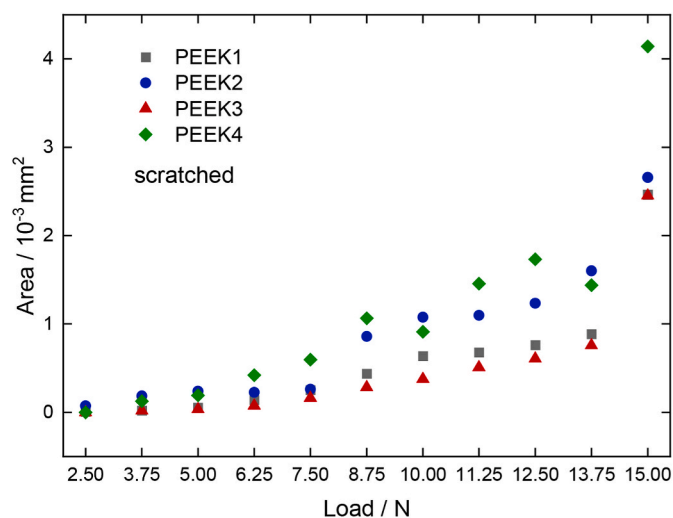


Fig. 11. The worn area formed due to the abrasion by Vicker's indenter.

of commercially available polyetheretherketones (PEEK) based materials for cryogenic applications were investigated. PEEK matrix was either modified or reinforced with carbon fibre, graphite and/or PTFE. Thermal properties were insignificantly affected by matrix modification. The addition of PTFE particles reduced the degree of crystallinity and thermal stability of PEEK, while reinforcement with carbon fibres, graphite and PTFE showed the opposite results. During the temperature reduction down to -170 °C, the prominent increment of storage modulus was observed for unfilled and PTFE reinforced PEEK, while addition of carbon fibres and graphite constrained the matrix contraction.

The mechanical properties were notably improved with addition of carbon fibres, graphite and PTFE, however, brittle fracture of the composites was observed during compression test. Fracture behaviour and impact strength were revealed to be dependent on the test temperature. The increase of impact strength was observed in β -relaxation region as a result of increased damping, $\tan \delta$, of the materials. Due to matrix shrinkage and reduced polymer chain mobility, the impact strength increased for unmodified polymers. Whilst impact strength of modified PEEK based materials was independent to temperature alteration. The toughening mechanism found for modified PEEK at 25 °C was hindered at -100 °C and -195 °C. Generally, matrix modification shifted the ductile/brittle fracture transition to lower temperatures.

In the scratch test with Vicker's indenter, the friction was found to be driven by the mechanical strength of the materials that effect the plastic deformation at the surface. The friction coefficient increased with the increase of the applied normal load reaching plateau at around 10 N. Test with the stainless-steel ball showed that friction was driven by the

adhesive forces and was independent to the increase of load. In PEEK composites, the fillers were found to act as load carriers until the load reached threshold values of 7 N, while above the 7 N, matrix deformation was predominant phenomena.

The modification of PEEK matrix showed improved mechanical properties at cryogenic temperatures over unmodified PEEK-based materials without significant effect on the thermal properties. The increased ductility of modified PEEK at cryogenic temperatures prevented brittle fracture, however, the impact toughness remained unchanged at the tested temperatures. The findings showed potential of the modified PEEK to be utilised in cryogenic sealing applications, for example, as a valve seats, where more stable thermal expansion coefficients and greater resilience at low temperatures are required. However, the tribological properties of the presented materials need to be studied in the future work.

CRedit authorship contribution statement

Maksim Nikonovich: Conceptualisation, Methodology, Analysis, Validation, Writing Original draft and editing Joana F. S. Costa: Investigation, Writing – Review and editing Ana C. Fonseca: Investigation, Writing – Review and editing Amilcar Ramalho: Conceptualisation, Supervision, Validation, Methodology Nazanin Emami: Conceptualisation, Supervision, Methodology, Validation, Writing – Review and editing.

Declaration of competing interest

The authors declare that they have no known competing financial interests or personal relationships that could have appeared to influence the work reported in this paper.

Data availability

Data will be made available on request.

Acknowledgement

The authors wish to acknowledge the European Union's Horizon 2020 research and innovation program under the Marie Skłodowska-Curie grant agreement No. 860246.

References

- R.R. Barth, K.L. Simmons, C. San Marchi, Polymers for Hydrogen Infrastructure and Vehicle Fuel Systems, vols. 1–51, Prod-Ng.Sandia.Gov, 2013. <https://prod-ng.sandia.gov/techlib-noauth/access-control.cgi/2013/138904.pdf>.
- T.F. Johnson, D.W. Sleight, R.A. Martin, Structures and design phase I summary for the NASA composite cryotank Technology demonstration project, in: 54th AIAA/ASME/ASCE/AHS/ASC Struct. Struct. Dyn. Mater. Conf., American Institute of Aeronautics and Astronautics, 2013. <https://doi.org/10.2514/6.2013-1825>.
- Fuel Cells and Hydrogen Joint Undertaking (FCH), Hydrogen Roadmap Europe, 2019. <https://doi.org/10.2843/249013>.
- I.A. Gondal, Hydrogen Transportation by Pipelines, Elsevier Ltd., 2016. <https://doi.org/10.1016/b978-1-78242-362-1.00012-2>.
- A. Turnbull, Hydrogen Diffusion and Trapping in Metals, Woodhead Publishing Limited, 2012. <https://doi.org/10.1533/9780857095374.1.89>.
- P.C. Michael, E. Rabinowicz, Y. Iwasa, Friction and wear of polymeric materials at 293, 77 and 4.2 K, *Cryogenics* 31 (1991) 695–704. [https://doi.org/10.1016/0011-2275\(91\)90230-T](https://doi.org/10.1016/0011-2275(91)90230-T).
- K. Friedrich, Polymer composites for tribological applications, *Adv. Ind. Eng. Polym. Res.* 1 (2018) 3–39. <https://doi.org/10.1016/j.aiepr.2018.05.001>.
- Q. Wang, F. Zheng, T. Wang, Tribological properties of polymers PI, PTFE and PEEK at cryogenic temperature in vacuum, *Cryogenics* 75 (2016) 19–25. <https://doi.org/10.1016/j.cryogenics.2016.01.001>.
- G. Theiler, W. Hübner, T. Gradt, P. Klein, K. Friedrich, Friction and wear of PTFE composites at cryogenic temperatures, *Tribol. Int.* 35 (2002) 449–458. [https://doi.org/10.1016/S0301-679X\(02\)00035-X](https://doi.org/10.1016/S0301-679X(02)00035-X).
- Z. Sági, R. Butler, Properties of cryogenic and low temperature composite materials – a review, *Cryogenics* 111 (2020), 103190. <https://doi.org/10.1016/j.cryogenics.2020.103190>.
- J.X. Chan, J.F. Wong, M. Petru, A. Hassan, U. Nirmal, N. Othman, R.A. Ilyas, Effect of nanofillers on tribological properties of polymer nanocomposites: a review on recent development, *Polymers* 13 (2021). <https://doi.org/10.3390/POLYMI13172867>.
- G. Hartwig, in: G. Hartwig (Ed.), *Polymers as Matrix for Composites BT - Polymer Properties at Room and Cryogenic Temperatures*, Springer US, Boston, MA, 1994, pp. 241–250. https://doi.org/10.1007/978-1-4757-6213-6_11.
- G. Theiler, T. Gradt, Friction and wear of polymer materials at cryogenic temperatures, in: S. Kalia, S.-Y. Fu (Eds.), *Polym. Cryog. Temp.*, Springer-Verlag, Berlin, 2013, pp. 41–58. <https://doi.org/10.1007/978-3-642-35335-2>.
- X.X. Chu, Z.X. Wu, R.J. Huang, Y. Zhou, L.F. Li, Mechanical and thermal expansion properties of glass fibers reinforced PEEK composites at cryogenic temperatures, *Cryogenics* 50 (2010) 84–88. <https://doi.org/10.1016/j.cryogenics.2009.12.003>.
- N. Soleimani, S.M. Khalili, R.E. Farsani, Z.H. Nasab, Mechanical properties of nanoclay reinforced polypropylene composites at cryogenic temperature, *J. Reinforc. Plast. Compos.* 31 (2012) 967–976. <https://doi.org/10.1177/0731684412450349/FORMAT/EPUB>.
- M. Askari, M. Javadi, R. Eslami-Farsani, A. Geranmayeh, Impact properties of carbon fibers-epoxy composite/aluminum laminates: effect of cryogenic and thermal aging, Iran, *Polym. J. (English Ed.)* 32 (2023) 187–201. <https://doi.org/10.1007/S13726-022-01116-X/FIGURES/12>.
- R.D. Adams, J.M. Gaitonde, Low-temperature flexural dynamic measurements on PEEK, HTA and some of their carbon fibre composites, *Compos. Sci. Technol.* 47 (1993) 271–287. [https://doi.org/10.1016/0266-3538\(93\)90036-G](https://doi.org/10.1016/0266-3538(93)90036-G).
- V.A. Bershtein, V.M. Egorov, *Differential Scanning Calorimetry of Polymers: Physics, Chemistry, Analysis, Technology*, Pearson Education, 1994.
- J. Wu, Y.W. Mai, B. Cotterell, Fracture toughness and fracture mechanisms of PBT/PC/IM blend - Part I Fracture properties, *J. Mater. Sci.* 28 (1993) 3373–3384. <https://doi.org/10.1007/BF00354261>.
- E. Plati, J.G. Williams, Effect of temperature on the impact fracture toughness of polymers, *Polymer (Guildf)* 16 (1975) 915–920. [https://doi.org/10.1016/0032-3861\(75\)90213-X](https://doi.org/10.1016/0032-3861(75)90213-X).
- P.I. Vincent, Impact strength and mechanical losses in thermoplastics, *Polymer (Guildf)* 15 (1974) 111–116. [https://doi.org/10.1016/0032-3861\(74\)90010-X](https://doi.org/10.1016/0032-3861(74)90010-X).
- D. Chen, J. Li, Y. Yuan, C. Gao, Y. Cui, S. Li, X. Liu, H. Wang, C. Peng, Z. Wu, A review of the polymer for cryogenic application: methods, mechanisms and perspectives, *Polymers* 13 (2021) 1–29. <https://doi.org/10.3390/polym13030320>.
- H. Voss, K. Friedrich, The wear behaviour composites, *Wear* 116 (1987) 1–18.
- R. Schroeder, F.W. Torres, C. Binder, A.N. Klein, J.D.B. De Mello, J.D.B. De Mello, Failure mode in sliding wear of PEEK based composites, *Wear* 301 (2013) 717–726. <https://doi.org/10.1016/j.wear.2012.11.055>.
- J. Karger-Kocsis, K. Friedrich, Temperature and strain-rate effects on the fracture toughness of poly(ether ether ketone) and its short glass-fibre reinforced composite, *Polymer (Guildf)* 27 (1986) 1753–1760. [https://doi.org/10.1016/0032-3861\(86\)90272-7](https://doi.org/10.1016/0032-3861(86)90272-7).
- Z. Rasheva, G. Zhang, T. Burkhart, A correlation between the tribological and mechanical properties of short carbon fibers reinforced PEEK materials with different fiber orientations, *Tribol. Int.* 43 (2010) 1430–1437. <https://doi.org/10.1016/j.triboint.2010.01.020>.
- A.P. Harsha, U.S. Tewari, The effect of fibre reinforcement and solid lubricants on abrasive wear behavior of polyetheretherketone composites, *J. Reinforc. Plast. Compos.* 22 (2003) 751–767. <https://doi.org/10.1177/0731684403022008005>.
- K. Friedrich, R. Walter, H. Voss, J. Karger-Kocsis, Effect of short fibre reinforcement on the fatigue crack propagation and fracture of PEEK-matrix composites, *Composites* 17 (1986) 205–216. [https://doi.org/10.1016/0010-4361\(86\)91004-9](https://doi.org/10.1016/0010-4361(86)91004-9).
- J.K. Lancaster, Relationships between the wear of polymers and their mechanical properties, *Proc. Inst. Mech. Eng. Conf. Proc.* 183 (1968) 98–106. https://doi.org/10.1243/pime_conf_1968_183_283_02.
- Z. Zhang, C. Breidt, L. Chang, K. Friedrich, Wear of PEEK composites related to their mechanical performances, *Tribol. Int.* 37 (2004) 271–277. <https://doi.org/10.1016/J.TRIBOINT.2003.09.005>.
- D.J. Blundell, B.N. Osborn, *The Morphology of Poly (Aryl-Ether-Ether- Ketone)*, 24, 1983, pp. 953–958.
- K. Tga, C. Fitting, P. Iv, Deconvolution of Thermal Analysis Data Using Commonly Cited Mathematical Models, (n.d.) 1–6.
- Y. Lee, R.S. Porter, Crystallization of Poly(etheretherketone) (PEEK) in Carbon Fiber Composites, (n.d.).
- J.N. Hay, D.J. Kemmish, Thermal decomposition of poly(aryl ether ketones), *Polymer (Guildf)* 28 (1987) 2047–2051. [https://doi.org/10.1016/0032-3861\(87\)90039-5](https://doi.org/10.1016/0032-3861(87)90039-5).
- P. Patel, T.R. Hull, R.W. McCabe, D. Flath, J. Grasmeder, M. Percy, Mechanism of thermal decomposition of poly(ether ether ketone) (PEEK) from a review of decomposition studies, *Polym. Degrad. Stabil.* 95 (2010) 709–718. <https://doi.org/10.1016/J.POLYMEDEGRADSTAB.2010.01.024>.
- L.H. Perng, C.J. Tsai, Y.C. Ling, Mechanism and kinetic modelling of PEEK pyrolysis by TG/MS, *Polymer (Guildf)* 40 (1999) 7321–7329. [https://doi.org/10.1016/S0032-3861\(99\)00006-3](https://doi.org/10.1016/S0032-3861(99)00006-3).
- P.R. Hondred, S. Yoon, N. Bowler, M.R. Kessler, Degradation kinetics of polytetrafluoroethylene and poly(ethylene-alt- tetrafluoroethylene), *High Perform. Polym.* 25 (2013) 535–542. https://doi.org/10.1177/0954008312473491/ASSET/IMAGES/LARGE/10.1177_0954008312473491-FIG2.JPEG.
- F. Li, Y. Hu, X. Hou, X. Hu, D. Jiang, Thermal, mechanical, and tribological properties of short carbon fibers/PEEK composites, (n.d.). <https://doi.org/10.1177/0954008317715313>.

- [39] F. Rezaei, R. Yunus, N.A. Ibrahim, Effect of fiber length on thermomechanical properties of short carbon fiber reinforced polypropylene composites, *Mater. Des.* 30 (2009) 260–263, <https://doi.org/10.1016/J.MATDES.2008.05.005>.
- [40] G.J. Farrow, G.H. Wostenholm, M.I. Darby, B. Yates, Thermal expansion of PEEK between 80 and 470 K, *J. Mater. Sci. Lett.* 9 (1990) 743–744.
- [41] S.X. Lu, P. Cebet, Thermal stability and thermal expansion studies of PEEK and related polyimides 37 (1996) 2999–3009.
- [42] Y.H. Lai, M.C. Kuo, J.C. Huang, M. Chen, On the PEEK composites reinforced by surface-modified nano-silica, *Mater. Sci. Eng. A.* 458 (2007) 158–169, <https://doi.org/10.1016/J.MSEA.2007.01.085>.
- [43] Joseph D. Menczel, R.B. Prime (Eds.), *Thermal Analysis of Polymers, Fundamental and Applications*, John Wiley & Sons, Inc., New Jersey, 2009.
- [44] J.P. Greene, J.O. Wilkes, Steady-State and dynamic properties of concentrated fiber-filled thermoplastics, *Polym. Eng. Sci.* 35 (1995) 1670–1681, <https://doi.org/10.1002/pen.760352103>.
- [45] H. Qu, W. Zhang, Z. Li, L. Hou, G. Li, J.Y. Fuh, W. Wu, Influence of thermal processing conditions on mechanical and material properties of 3D printed thin-structures using PEEK material, *Int. J. Precis. Eng. Manuf.* 23 (2022) 689–699, <https://doi.org/10.1007/S12541-022-00650-1/FIGURES/10>.
- [46] Y. Niu, S. Zheng, P. Song, X. Zhang, C. Wang, Mechanical and thermal properties of PEEK composites by incorporating inorganic particles modified phosphates, *Compos. Part B Eng.* 212 (2021), 108715, <https://doi.org/10.1016/J.COMPOSITESB.2021.108715>.
- [47] S.L. Gao, J.K. Kim, Correlation among crystalline morphology of PEEK, interface bond strength, and in-plane mechanical properties of carbon/PEEK composites, *J. Appl. Polym. Sci.* 84 (2002) 1155–1167, <https://doi.org/10.1002/APP.10406>.
- [48] W. Hübner, T. Gradt, T. Schneider, H. Börner, Tribological behaviour of materials at cryogenic temperatures, *Wear* 216 (1998) 150–159, [https://doi.org/10.1016/S0043-1648\(97\)00187-7](https://doi.org/10.1016/S0043-1648(97)00187-7).
- [49] G. Theiler, *PTFE- and PEEK-Matrix Composites for Tribological Applications at Cryogenic Temperatures and in Hydrogen*, BAM, 2005.
- [50] J.G. Williams, J.M. Hodgkinson, Crack-blunting mechanisms in impact tests on polymers, in: *Proc. R. Soc. Lond. A. Math. Phys. Sci.*, Royal Society, 1981, pp. 231–247. <http://www.jstor.org/stable/2414705>.
- [51] J. Heijboer, Dynamic mechanical properties and impact strength, *J. Polym. Sci. PART C NO. 16* (1968) 3755–3763, <https://doi.org/10.1002/polc.5070160716>.
- [52] Y. Wada, T. Kasahara, Relation between impact strength and dynamic mechanical properties of plastics, *Appl. Polym. Sci.* 11 (1967) 1661–1665, <https://doi.org/10.1002/app.1967.070110906>.
- [53] L.J. Broutman, S.M. Krishnakumar, Impact strength of polymers: 1. The effect of thermal treatment and residual stress, *Polym. Eng. Sci.* 16 (1976) 74–81, <https://doi.org/10.1002/pen.760160203>.
- [54] S. Zhou, Q. Zhang, C. Wu, J. Huang, Effect of carbon fiber reinforcement on the mechanical and tribological properties of polyamide6/polyphenylene sulfide composites, *Mater. Des.* 44 (2013) 493–499, <https://doi.org/10.1016/J.MATDES.2012.08.029>.